Intraoperative localized constrained registration in navigated bronchoscopy

5 Erlend Fagertun Hofstad (MSc)[1], Hanne Sorger (MD)[2,3], Janne Beate Lervik Bakeng (MSc) [1], Lucian Gruionu (PhD)[4], Håkon Olav Leira (MD, PhD)[2,3], Tore Amundsen (MD, PhD)[2,3], Thomas Langø (PhD)[1]

10

[1] Department of Medical Technology, SINTEF Technology and Society, Trondheim, Norway
[2] Dept. Thoracic Medicine, St. Olav's Hospital, Trondheim, Norway
[3] Department of Circulation and Medical Imaging, Faculty of Medicine, Norwegian
15 University of Science and Technology (NTNU), Trondheim, Norway
[4] Department of Automotive, Transportation and Industrial Engineering, Faculty of Mechanics, University of Craiova, Romania

20

25

30

Corresponding author:
35 Erlend Fagertun Hofstad, MSc, Research Scientist
SINTEF Technology and Society
Dept. of Medical Technology
PB 4760 Sluppen
7465 Trondheim, Norway
40 Phone: +47 911 96 173
Fax: +47 93 07 08 00
e-mail: erlend.hofstad@sintef.no

45

Abstract

Purpose

One of the major challenges in electromagnetic navigated bronchoscopy is the navigation accuracy. An initial rigid image-to-patient registration may not be optimal for the entire lung volume, as the lung tissue anatomy is likely to have shifted since the time of computer tomography (CT) acquisition. The accuracy of the initial rigid registration will also be affected throughout the procedure by breathing, coughing, patient movement and tissue displacements due to pressure from bronchoscopy tools. A method to minimize the negative impact from these factors by updating the registration locally during the procedure is needed and suggested in this paper.

Methods

The intraoperative local registration method updates the initial registration by optimization in an area of special interest, e.g. close to a biopsy position. The local registration was developed through an adaptation of a previously published registration method used for the initial registration of CT to the patient anatomy. The method was tested in an experimental breathing phantom setup, where respiratory movements were induced by a robotic arm. Deformations were also applied to the phantom to see if the local registration could compensate for these.

Results

The local registration was successfully applied in all 15 repetitions, 5 in each of the three parts of the airway phantom. The mean registration accuracy was

improved from 11.8 – 19.4 mm to 4.0 – 6.7 mm, varying to some degree in the different segments of the airway model.

Conclusions

75 A local registration method, to update and improve the initial image-to patient registration during navigated bronchoscopy, was developed. The method was successfully tested in a breathing phantom setup. Further development is needed to make the method more automatic. It must also be verified in human studies.

80

85

Introduction

Bronchoscopy is used for endoluminal inspection and diagnostic procedures in the lungs. It is the essential diagnostic tool when investigating lung lesions that

90 could represent malignant tumors. Precise navigation of the flexible bronchoscope through the airways to a defined target is challenging due to the numerous divisions and the lack of direct visibility of lesions in the lung periphery. The diagnostic success rate in bronchoscopy for non-visible tumors can be as low as 10-15%, depending on tumor localization, size, the experience of

95 the pulmonologist, and the method used for obtaining tissue specimen, compared to 80-90% for visible tumors [1-3].

In electromagnetic navigated bronchoscopy (ENB), the instruments may be traced by attaching an electromagnetic (EM) sensor to the tip of the

100 bronchoscope and tools for tissue sampling. The positions of the instruments are furthermore displayed on maps made from preoperative images of the patient, e.g. computer tomography (CT). Using ENB to reach non-visible tumors in the lung has increased the diagnostic yield to 70-80 % [4]. Commercially available systems like superDimension™ Navigation System (Covidien, Inc., Minneapolis,

105 USA) and SPiN® Thoracic Navigation System (Veran Medical Technologies, Inc., St. Louis, USA) provide navigation based on electromagnetic tracking (EMT) of the bronchoscopic tools. Alternative tracking techniques for navigated bronchoscopy has also been tested, such as externally mounted sensors for measurement of endoscope insertion depth, rotational angel and tip bending

110 angle [5]. A detailed description of the existing commercial and research systems

4

for navigated bronchoscopy can be found in Reynisson et al. [6].

Preoperative registration of the CT images to the patient anatomy is one of the essential steps to achieve adequate sampling accuracy with the ENB technology.

115   The registration procedure can either be conducted using the EMT system, by image based registration [7] or a combination of both [8, 9]. Registration methods using information from the EMT system can furthermore be divided into landmark [8, 10] or centerline based approaches. Centerline based methods matches the shape and exact location of the airways extracted from the CT

120   images to the positions of the bronchoscope sampled while advancing through the airways. Centerline based registration methods have been presented by Deguchi *et al.* [11, 12], Mori *et al.* [13] and Feuerstein *et al.* [14]. Our group have previously suggested an automatic centerline based registration method [15], which utilizes both the positions and orientations of the bronchoscope and the

125   airway centerline from the CT images in the registration process. The previously published method was compared to the registration method of Feuerstein et al [14] by using simulated data, and similar results were found [15]. The method was also shown to function to its purpose on data acquired from patients. The registration method was implemented in our open source research navigation

130   platform, CustusX [1], and successfully used in ENB procedures on patients [16].

The rigidity of the method is a drawback. It does not handle anatomical deformations from the CT, which is acquired during a short segment of the respiratory cycle, often several days or even weeks ahead of the procedure.

135   Enlargement of tumor or lymph nodes from the time of CT acquisition may also

impact the anatomy. Lung tissue and airway movement due to breathing and coughing cause further complications to the registration, and can result in local variations in the navigation accuracy. During the bronchoscopy procedure, after the initial registration, a consciously sedated patient might move on the

140　operating table, and the movement measured by e.g. a sensor on the patient's chest, will not necessarily be transferable to the displacement inside the lungs. Pressure from the bronchoscope itself may also deform the lung tissue compared to the CT images [17].

145　A dynamically updated registration could reduce the negative effects from these factors. We have by adaptation of the registration method presented in [15], developed a local registration to be used during bronchoscopy, intended to compensate for anatomic transformations and deformations. To our knowledge, a registration method to optimize the accuracy in an area of interest, e.g. close to

150　a tumor, has not previously been suggested. The registration can be updated during the procedure, and thus compensate for anatomic deformations from CT acquisition to the bronchoscopy, or anatomic shifts and/or deformations during the procedure.

155　To test the new registration method, we adapted a commercially available lung airway phantom and simulated breathing motions to the phantom in a robotic setup. This allowed testing of the method with realistic breathing and other potentially appearing influences. We also induced deformations to the airway model to assess the local registration method.

160

Materials and Methods

Local registration method

The local registration method suggested in this paper is based on a previously published global registration method [15]. The new method is, as the initial

165   registration, a rigid method, but the dataset is reduced to a segment of the airways instead of the entire airway structure. The intention is to perform a local registration correction during bronchoscopy to improve the navigation accuracy. Before a local registration can be conducted, an initial registration of the CT data to the patient is required. This is performed by maneuvering the bronchoscope

170   through the bronchi, normally during the initial part of bronchoscopy while applying topical anesthetics, and running the registration method described in [15], by matching bronchoscope positions to the airways centerline from preoperative CT. This results in a transformation, $^{CT}T_{EM}$, between the EMT and the CT coordinate systems. This registration initializes the local registration:

175

$$^{CT}T^{Local}_{EM} = {}^{CT}T_{EM} \tag{1}$$

In the local registration method, positions from the EMT sensor at the tip of the bronchoscope is acquired while it is maneuvered through airway bronchi close

180   to the area of interest, e.g. a lymph node or tumor in which a transbronchial needle aspiration (TBNA) is to be performed. To compensate for variations in the speed at which the bronchoscope is advanced, and thus the distribution of the recorded tip positions, a filter ensures that only positions at a Euclidean distance of >1 mm from the last included position are used in the local registration.

185

In the registration method presented in [15], all positions in the CT centerline
were used as input. In the local registration procedure, only CT centerline
positions close to the acquired bronchoscope tip positions are used. A filter
selects CT centerline positions at a certain distance from any of the recorded

190   bronchoscope tip positions. This distance was set to 20 mm in this study, which
has proven to be a value large enough to compensate for typical local variations.

An iterative closest point (ICP) registration algorithm is then run matching these
tracking data with the centerline of the airways, which is extracted from the CT

195   images prior to the procedure. In an ICP algorithm the distance between two
clouds of points, in this case the EMT positions of the bronchoscope tip and the
CT centerline, is minimized by transforming (translation and rotation) one of the
clouds of points. In the registration algorithm we have utilized, in addition to the
distances, the orientations of the bronchoscope by matching it to the running

200   direction of the CT centerline (equation 4). A good correspondence between the
orientation of the bronchoscope and the running direction of the centerline is an
indication that the correct set of branches is matched. The combined Euclidian
and orientation distance between the EMT positions of the bronchoscope tip and
the CT centerline is calculated by:

205

$$d_c^{j,k} = d_p^{j,k} + \alpha^j \cdot d_o^{j,k} \tag{2}$$

$$d_p^{j,k} = \left\| {}^{CT}T_{EM}^{Local} \cdot {}^{BT}p^j - {}^{CT}p^k \right\| \tag{3}$$

210 $$d_o^{j,k} = \left\| {}^{CT}T_{EM}^{Local} \cdot {}^{BT}o^j - {}^{CT}o^k \right\| \tag{4}$$

$$\alpha^j = \sqrt{\frac{1}{N}\sum_{k=1}^{N}\frac{d_p^{j,k}}{d_o^{j,k}}} \tag{5}$$

where p is position, o is orientation, c is combined, BT is bronchoscope tip, CT is

215 CT centerline, and j and k are the sample indices of the bronchoscope tip and CT

centerline points. α is a weighting factor between the deviation in position and

the deviation in orientation for all possible point pairs in the two datasets. Using

the α factor ensures that both the Euclidian distance and orientation are

significant components in the combined distance independent of the Euclidian

220 distance.

Each bronchoscope position (j) is paired to the centerline position (k) at the

smallest combined distance:

225 $$d_c^{j,k_j} = \arg\min_k d_c^{j,k} \tag{6}$$

A small deviation between the orientation of the bronchoscope and the running

direction of the centerline indicates that the corresponding branches in the two

datasets are matched. To increase the likelihood of bronchoscope positions being

230 paired with centerline positions from the corresponding branch, we select a

partition (70%) of the bronchoscope positions with the smallest orientation

deviation (d_o^{j,k_j}) from its paired centerline position to serve as input to the paired-point registration. The next iteration of the calibration matrix is found by:

235
$$^{CT}T_{EM^*} = \arg\min_{^{CT}T'_{EM^*}} \sum_{j=1}^{N} \left\| {}^{CT}T'_{EM^*} \cdot {}^{CT}T_{EM}^{Local} \cdot {}^{BT}p^j - {}^{CT}p^{k_j} \right\| \tag{7}$$

which is calculated using a closed-form method [18].

The local registration is then updated:

240
$$^{CT}T_{EM}^{Local} = {}^{CT}T_{EM^*} \cdot {}^{CT}T_{EM}^{Local} \tag{8}$$

before the next iteration of the algorithm, starting at equation (2). The algorithm is run until the registration matrix, $^{CT}T_{EM}^{Local}$, converges.

245

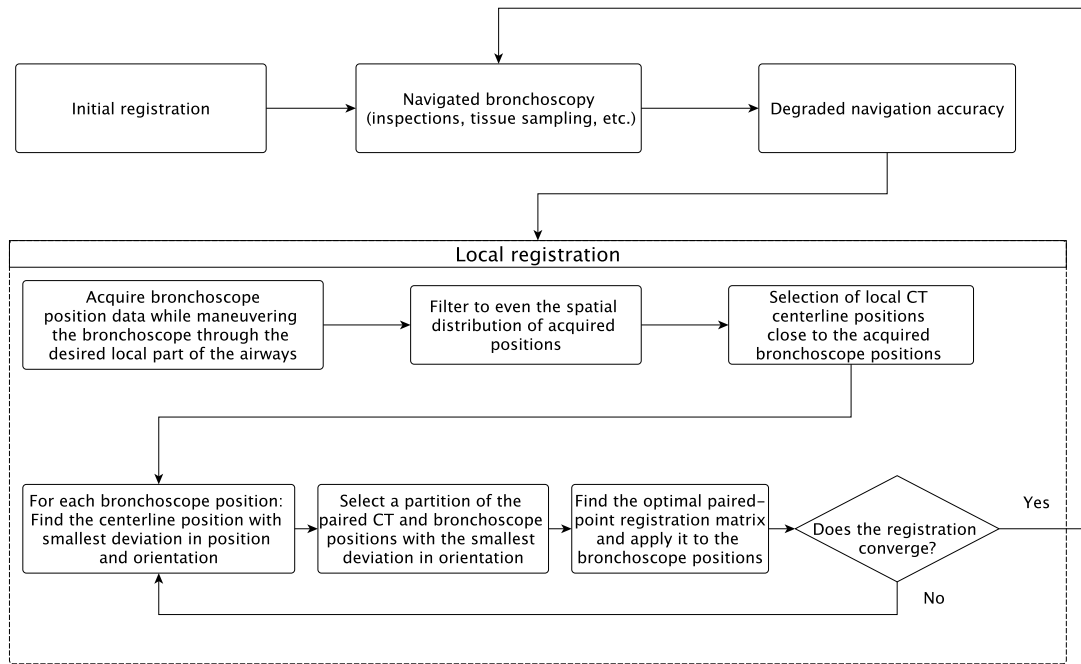An overview of the steps in the local registration algorithm is presented in Fig. 1.

Figure 1: The steps in the local registration method.

250

Phantom setup

For the experiment, we used an airway phantom, the Ultrasonic Bronchoscopy

Simulator LM-099 (KOKEN CO., LTD, Tokyo, Japan). To make the phantom CT

compatible, it was transferred from its original container into a plastic box, and

255   all metal parts were replaced with plastic. In total ten markers, Tantalum balls (D

= 0.8 mm, Tilly Medical Products AB, Lund, Sweden), were attached to the

outside of the airway wall. The markers can easily be identified both in the CT

images and in physical space. CT images were acquired using a thorax lung scan

protocol with 631 slices of 512x512 pixels, element spacing 0.752x0.752x0.499

260   mm, and slice thickness 1.0 mm.

The airway model was divided into three local parts for the phantom

experiments: right lung (RL) (markers 1-4 in Fig. 2), left upper lobe (LUL)

(markers 5-7) and left lower lobe (LLL) (markers 8-10). With this setup it was

265   possible to compare the registration results in an entire lung, RL, to the results in

lung segments, LUL and LLL. Comparing the results in LUL and LLL was intended

to demonstrate the difference between central and peripheral parts of the

airways.
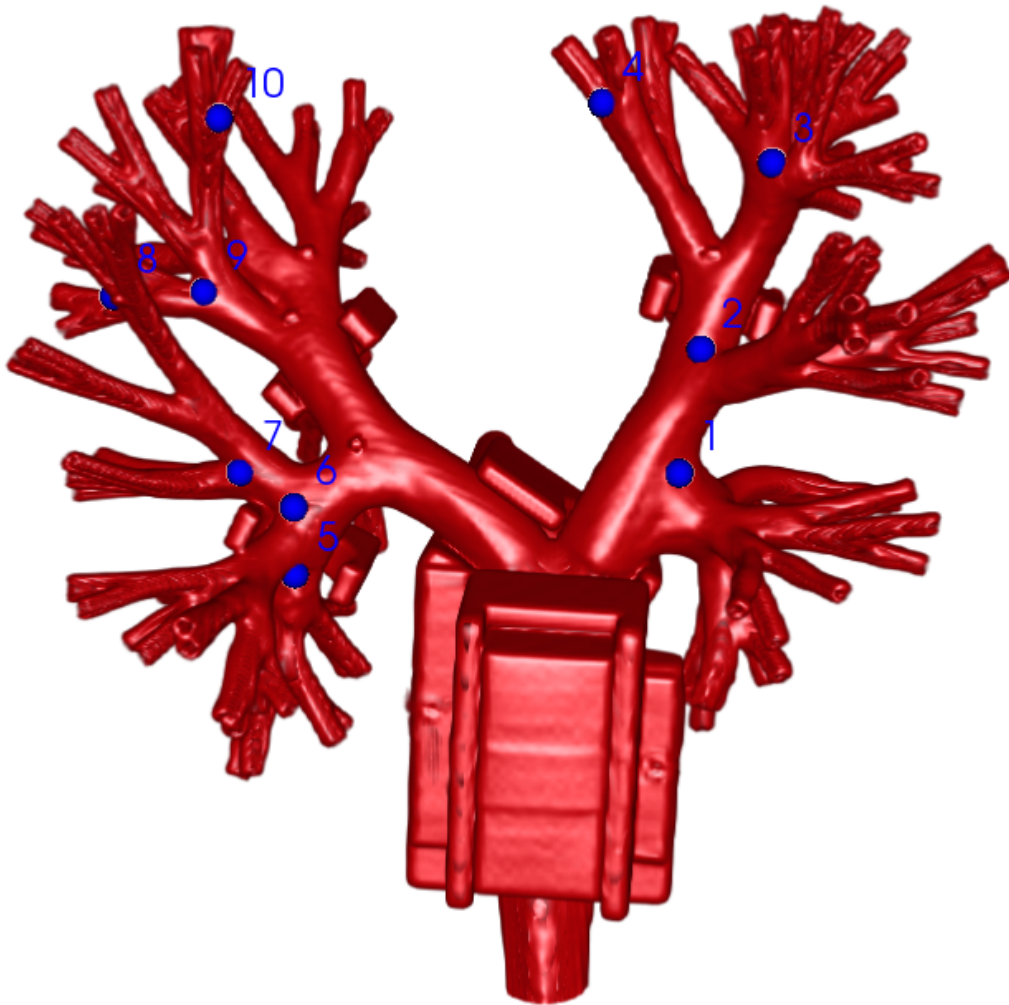
270

Figure 2: A 3D model (from CT images) of the phantom and the Tantalum ball marker

positions.

We used a robotic arm to induce motions to the airway phantom, similar to

275   human breathing, see Fig. 3. The UR5-robot (Universal Robots, Odense,

Denmark) was connected to the airway phantom using rubber bands. The robot

was programmed to move 50 mm in the inferior/superior direction to simulate

breathing cycles with respiration frequency of 12 breaths per minute: 1.5

seconds inspiratory motion, 1.5 seconds expiratory motion and 2 seconds pause
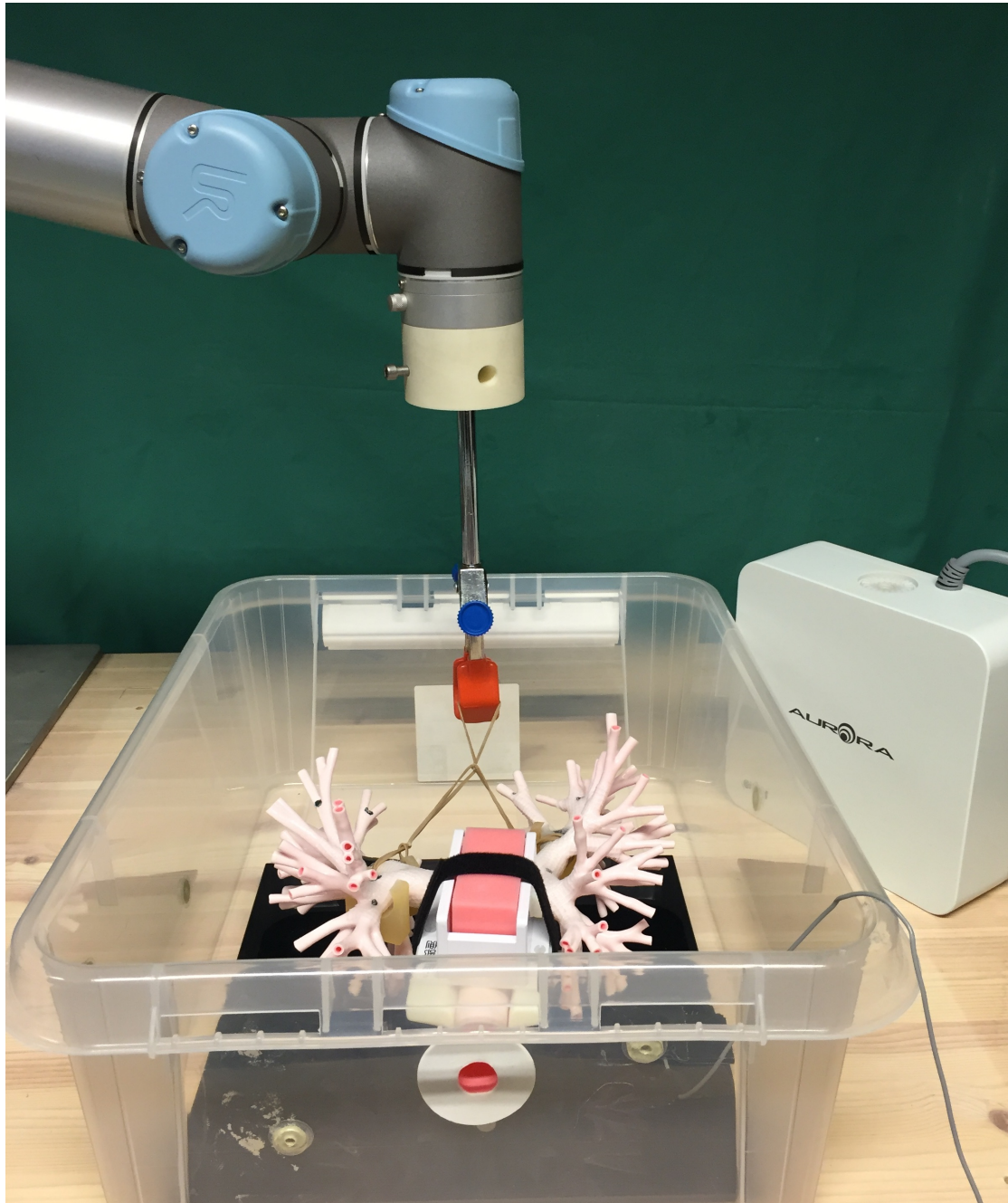
280   after exhale.

Figure 3: The experimental setup with a robotic arm inducing respiratory motions to the airway phantom. The EMT field generator is placed to the right of the phantom.

285

Navigation system

290   The open source navigation research platform, CustusX [1] (SINTEF, Trondheim, Norway, www.custusx.org), was used in the experiments. The system can import preoperative radiology images and stream real-time images, such as ultrasound. Information from the images is combined with EM or optical tracking systems. The local registration method presented in this paper is implemented in CustusX.

295   We used the Aurora® EMT System (Northern Digital Inc., Waterloo, ON, Canada). The field generator unit was placed on the right side of the phantom, as shown in Fig. 3. A position sensor with six degrees of freedom (DOF) (Northern Digital Inc., Waterloo, ON, Canada) was attached close to the tip of the bronchoscope (Fig. 4). The CT DICOM data was imported into CustusX, and the airways and its

300   centerline were extracted using the automatic method described in [19]. The positions of the Tantalum ball markers were sampled in the CT images. The physical positions of the markers were sampled by using an EMT pointer (Aurora 6DOF Probe, Straight Tip, Standard, Northern Digital Inc., Waterloo, ON, Canada).

305

Figure 4: The bronchoscope with a position tracking sensor mounted close to the tip.

Accuracy calculation

310   The accuracy was calculated by comparing the CT position of each of the Tantalum ball marker to the physical position measured by an EMT pointer. The physical positions of the Tantalum ball markers were measured at both inspiration and expiration position by pausing the robotic breathing motion. Each marker's position was calculated assuming linear movement at constant

315   velocity during the breathing cycle. The deviation from the markers CT position was then found, and the average accuracy from all markers was calculated:

Navigation accuracy: $\frac{1}{N}\sum_{i=1}^{N}\left\|p_{CT}^{i} - \tilde{p}_{EM}^{i}\right\|$ (9)

320 $$\tilde{p}_{EM}^i = \frac{1}{5s}\left((1.5s + 1.5s)\frac{p_{EM_{inhale}}^i + p_{EM_{exhale}}^i}{2} + 2s * p_{EM_{exhale}}^i\right) \qquad (10)$$

where p is the positions measured in the CT volume (CT) or by the EMT pointer (EM), and i is the number of the Tantalum ball marker.

Experiment
325

Breathing movement measurement

The size of the breathing motions in the lung model was measured by pausing the robot at both end inspiration and end expiration position. The Tantalum ball markers were pinpointed using the EMT pointer at both robot positions.

330

Initial registration

An initial registration was performed by acquiring positions of the bronchoscope tip while maneuvering the bronchoscope through the lumen of the lung model, and applying the registration method described in [15]. The phantom breathing

335   was enabled during the registration process.

Deformation

Local deformations were applied by displacing parts of the lung model, by moving the robot in the anterior/posterior and medial/lateral direction. The

340   robot was moved 20-40 mm. The movement of the phantom airways was lower

due to the connection through the elastic rubber bands. The navigation accuracy was measured after the deformation.

Local registration

345   After the deformation, a local registration was applied to one of the three parts of the lung model, RL, LUL or LLL. In total 15 local registrations were performed, five to each part. The navigation accuracy was measured again and compared to the accuracy before local registration, both with and without deformation.

350   **Results**

Breathing movement measurement

The mean breathing motion measured at the ten Tantalum ball markers was 7.7 mm (max: 16.0 mm, min: 2.8 mm). This is illustrated in Fig. 5 where the end inspiratory and end expiratory positions are plotted in a 2D projection view, on

355   top of the centerline of the airways. The displacement for each marker and mean displacement for each subpart of the phantom is presented in Table 1. The peripherally located markers (2-4, 8-10) are more affected by the breathing motions (mean 10.5 mm) than the markers in the upper lobes (1, 5-7) (mean 3.5 mm).
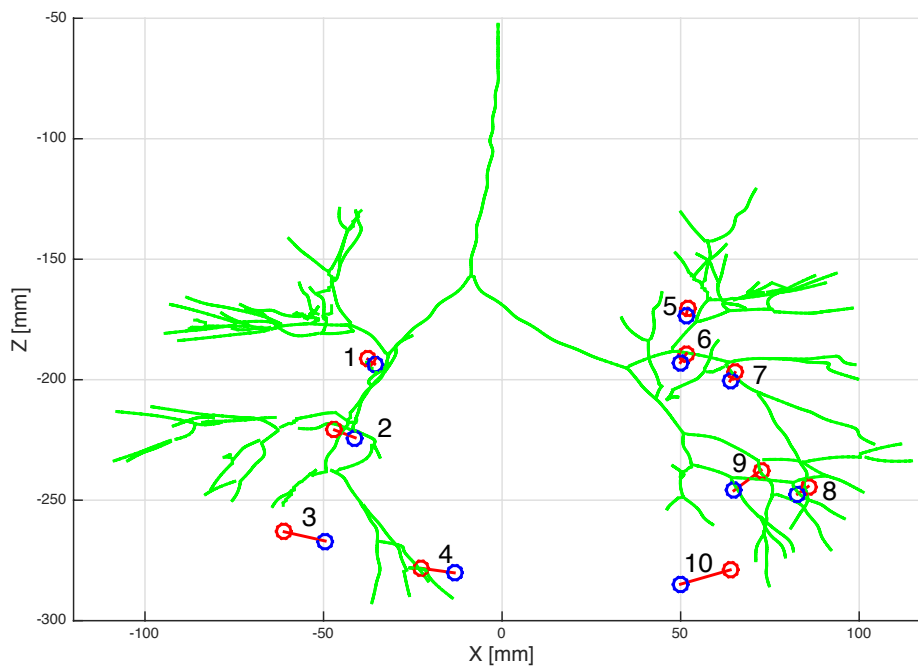
360

Figure 5: A 2D frontal view of the Tantalum ball markers' displacement from respiratory movements. The markers (1-10) at end-inhale (blue) and end-exhale (red) position. The airway centerline from the CT of the phantom in green.

Table 1: The displacement of each of the 10 Tantalum ball markers from respiratory movements, and the mean displacement for the markers in each subpart of the phantom

Part	Marker no.	Displacement (mm)	Mean displacement each part (mm)
Right lung	1	2.8	
	2	6.7	
	3	12.1	RL:
	4	9.7	7.8
Left upper lobe	5	3.0	
	6	4.2	LUL:
	7	4.0	3.7
Left lower lobe	8	6.6	
	9	12.1	LLL:
	10	16.0	11.6
	Mean (mm):	7.7	

Initial registration

The bronchoscope tip positions for the initial registration were acquired in 114 seconds, while the bronchoscope was maneuvered through totally 14 airway branches. The navigation accuracy for all ten Tantalum ball markers after the

380   initial registration was measured to 5.4 ± 3.1 mm (Table 2), when using the mean inhale-exhale value as described in *Materials and Methods*, *Accuracy Calculation*. The theoretical optimal registration for these positions was found to be 4.1 ± 2.0 mm by applying a closed form paired-point registration [18] to the two sets of Tantalum ball marker positions (from CT and EMT).

385   The navigation accuracy for each of the three parts of the lung (RL, LUL and LLL) is shown in Table 2.

Table 2: The navigation accuracy after initial registration at each of the ten marker

positions, and mean accuracy for the marker positions included in each part of the lung

and for all positions totally.

Part	Marker no.	Mean (mm)	Mean accuracy each part (mm)
Right lung	1	1.6	
	2	1.6	
	3	6.0	RL:
	4	6.0	3.8
Left upper lobe	5	3.8	
	6	4.5	LUL:
	7	3.7	4.0
Left lower lobe	8	8.1	
	9	7.2	LLL:
	10	11.7	9.0
	Mean (mm):	5.4	

Deformation

Three different deformations were applied to each of the three parts of the lung

400   phantom by shifting the robots expiration and inspiration position. The resulting

accuracy after the deformation was 5.9-14.4 mm in RL, 7.7-11.8 in LUL and 11.6-

30.6 in LLL (Table 3-5).

Local registration

405   In total 15 local registrations were performed, by maneuvering the

bronchoscope at the part of the lung deformed. The positions for the local

registrations were acquired in 22 – 69 seconds (880-2760 acquired positions at

40 Hz sampling rate), while maneuvering the bronchoscope through 4-6

branches. The processing time of the registration algorithm was <1 second.

410   Figure 6 shows an example of a local registration in the LUL and how the

acquired bronchoscope tip positions and Tantalum ball marker positions are

changed.

The navigation accuracy was measured both before and after the local

415   registration (Table 3-5). All local registrations resulted in improved navigation

accuracy. From a mean accuracy of 11.8 mm, 12.2 mm and 19.4 mm to 6.0 mm,

4.0 mm and 4.7 mm in RL, LUL and LLL respectively. For 7 of 15 local

registrations the accuracy was even better than before the deformation (after

initial registration). In the two smallest local regions, the mean accuracy after

420   local registration was the same (4.0 mm LUL) or better (9.0 – 6.7 mm in LLL)

than before deformation.

425   Table 3: Right lung (RL): The navigation accuracy for local registration 1-5.

Repetition no.	1	2	3	4	5
Acquisition time (seconds)	58	42	43	39	22
Accuracy after deformation	5.9	10.0	14.4	14.4	14.4
Accuracy after local registration	3.1	7.9	5.9	7.1	6.0

Mean accuracy	After initial registration:	3.8	After deformation:	11.8	After local registration:	6.0

Table 4: Left upper lobe (LUL) results: The navigation accuracy for local registration 6-10.

Repetition no.	6	7	8	9	10
Acquisition time (seconds)	32	47	52	59	65
Accuracy after	7.7	17.9	11.8	11.8	11.8

deformation					
Accuracy after					
local registration	4.3	6.2	2.8	2.5	4.4

Mean accuracy	After initial registration:	4.0	After deformation:	12.2	After local registration:	4.0

430

Table 5: Left lower lobe (LLL) results: The navigation accuracy for local registration 11-15.

Repetition no.	11	12	13	14	15
Acquisition time (seconds)	61	36	52	43	69
Accuracy after deformation	11.6	30.6	18.3	18.3	18.3
Accuracy after local registration	6.5	7.3	6.2	4.8	9.5

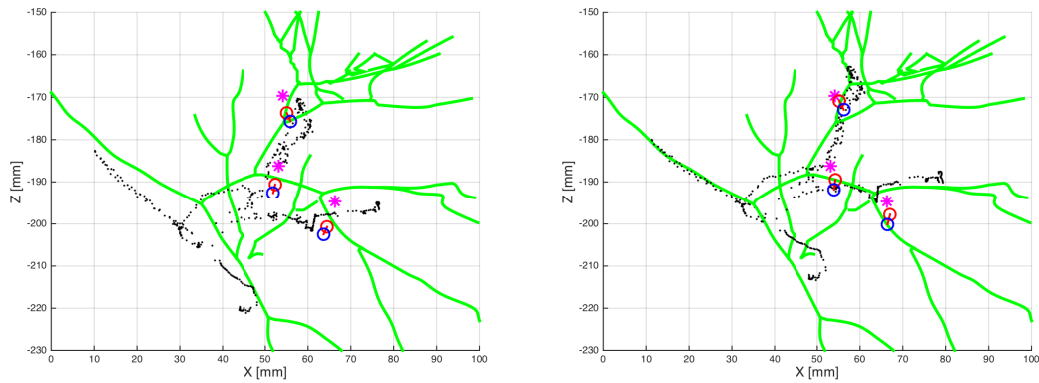| Mean accuracy	After initial registration:	9.0	After deformation:	19.4	After local registration:	6.7

435

Figure 6: A zoomed 2D frontal view local registration in the LUL (experiment no. 6), before (left) and after (right) registration. The centerline of the airways from CT in green and the positions of the sensor at the tip of the bronchoscope in black. The markers at end-inhale (blue circle) and end-exhale (red circle) position, and CT position (magenta star).

Discussion

A novel, intraoperative method for updating the CT-to-patient registration locally during ENB has been developed and demonstrated. The method was tested on an airway phantom connected to a robot simulating breathing motions. To our knowledge, this technique of updating the image–to-patient registration locally using a centerline based method in ENB has not been presented before.

The breathing motions of the lung phantom was measured to 7.7 mm on average, which is slightly smaller than an average motion of 10 mm described in other studies [17, 20]. Especially in the upper lobes the motions created by the robot were smaller than what was reported by Zhang et al.[20], 7.2 mm vs. 3.5 mm. The breathing motions could also have been made more realistic by including a

26

455   small random length in the extent of the inspiration/expiration. Motions

simulating the patient coughing could also be included in a more advanced setup.

The EM tracking system is vulnerable to surrounding metal, affecting the

accuracy. In this study, part of the robotic arm was within the EM field and could

460   potentially have an impact on the tracking system accuracy. However, we believe

this is not unrealistic compared to the situation in the bronchoscopy suite, where

equipment used both in and close to the EM field contains metal, even though it

is avoided as far as possible in navigated bronchoscopy using EMT. It is possible

that the local registration is less vulnerable to disturbances causing

465   deformations to the EM field, as the deformations most likely are relatively small

within a limited local area of the lungs.

The average initial registration error was 5.4 mm, while the theoretically lowest

average registration error was 4.1 mm. The main reasons for the optimal

470   registration accuracy not being closer to zero are deformation in the soft and

flexible airways from the CT acquisition to the phantom setup and deformations

caused by the breathing motions. Using a more rigid lung model or encapsulating

the airways in a flexible material (e.g. gelatin) would result in less deformation

from CT to experiment. However, some anatomical variations from CT

475   acquisition to bronchoscopy can be expected in humans as well. The initial

registration error is higher than found by simulated data using the same method

[15], but comparable to the average fiducial error in a similar breathing phantom

study, using a different centerline registration algorithm (5.8 mm) [21].

480   The local registration was successfully performed by acquiring positions of the

        bronchoscope tip while maneuvering the scope in a subset of the airway

        branches and matching it to the centerline of the same airways extracted from

        the CT volume of the phantom. All 15 registrations improved the navigation

        accuracy, and for seven of the registrations the accuracy was even better than

485   after the initial registration. The results after local registration were better in

        LUL than LLL and RL. The lower accuracy in the LLL was likely caused by the

        larger breathing motion and larger deformations compared to LUL. On the other

        hand, the accuracy improvement was highest in LLL. The accuracy after local

        registration in RL was probably affected by the larger area covered by the RL

490   markers, causing a high variation in the accuracy after initial registration and

        more inhomogeneity regarding both deformation from CT to experiment and

        from breathing motions. From this it appears as a more limited region than one

        entire lung (left or right) should be included in the local registration.

495   In the calculation of the accuracy (CT to EMT deviation), we used the average

        position of each Tantalum ball on the phantom. The average position was found

        by measuring the position at end inhale and exhale, and assuming linear

        movement at constant speed. Due to the elasticity of the rubber bands used to

        connect the robot to the airways, the assumption of constant speed is probably

500   not correct, however this has a very limited effect on the average position. It

        should be noted that a CT scan is normally performed while the patient is

        holding the breath after inhaling. This phantom scan was acquired in the end

        exhale state, as the airways was pulled by the robot in the inferior direction to

        form the end inhale position. This might have a minimal effect on the registration

505   result as the breathing motion pauses in the end exhale state, and thus the EMT

position is more weighted to the same state as in the CT volume compared to a

real human bronchoscopy setting.

The main requirement for the local registration method to function to its

510   purpose lies in matching the correct branches from EMT and CT. To maximize

the likelihood of a correct match, the algorithm utilizes information about the

orientation of the branches. I addition, the method searches for branches in the

close approximation to the acquired EMT positions, eliminating the risk of

matching it to e.g. branches in the opposite lung with similar orientations. In our

515   experiment the bronchoscope tip was moved through 4-6 branches in 22-69

seconds for the local registration. By comparing the length of the acquisitions

with the registration accuracy in Table 3-5, there is no indication of a longer

acquisition resulting in better accuracy. It is likely to be more important that the

registration acquisition covers branches in which the deviation in the orientation

520   is sufficiently large. I.e. the method is more likely to succeed if the bronchoscope

makes large turns whilst acquiring positions.

One could argue that a deformable initial registration would be a possible

solution to compensate for deformations in patient anatomy from CT acquisition

525   to the bronchoscopy. This approach would, however, not be valid throughout the

procedure if e.g. the patient is moving slightly or the instruments are affecting

the position of the lung tissue. A deformable registration approach does not

necessarily improve the alignment outside the airways included in the

registration either, e.g. other airways or a biopsy position. Vijayan et al. [22]

530   showed this in a porcine model study where deformations in the liver was

attempted compensated for by both rigid and deformable vessel centerline

registration. The centerline were better aligned using deformable registration.

However, this was not transferable to tumor models in the liver, which were best

aligned using only the rigid part of the centerline registration.

535

Different approaches have previously been suggested to update the image-to-

patient registration in bronchoscopy. The position of the bronchoscope can be

projected to the nearest centerline [10] with the risk of projection to the wrong

position on the centerline or even an adjacent branch. An alternative approach to

540   perform local corrections is imaged-based registration [8, 9], by matching the

camera image to the CT image. This approach is, however, only valid for tracking

the bronchoscope itself and cannot be used to update the position of tools

deployed into the periphery of the airways from the working channel of the

bronchoscope.

545

The suggested method in this paper has potential to improve the clinical

application of navigated bronchoscopy, by ensuring improved local accuracy and

robustness by correction of anatomical shifts or deformations. However, further

development of the presented local registration method should include making it

550   more automatic, by e.g. dynamically using the latest positions of the

bronchoscope or other navigated tools like a biopsy forceps to update the

registration when necessary. The method also needs to be tested in human

studies to verify its accuracy and robustness, and to identify and resolve

potentially practical complications.

Conclusion

We have developed a novel local registration method for ENB, which compensates movements or anatomical deformations during the ENB procedure or from CT acquisition to the procedure. The method was tested successfully in a

560   phantom setup, where a robot induced motions mimicking breathing. Further development should be made to make the method more automatic, requiring very limited or no input from the operator of the navigation system. The method should also be verified in a human ENB study.

Conflict of interests

575   The authors declare that they have no conflict of interest.

References

1. Askeland C, Solberg OV, Bakeng JB, Reinertsen I, Tangen GA, Hofstad EF, Iversen DH, Vapenstad C, Selbekk T, Lango T *et al*: CustusX: an open-source research platform for image-guided therapy. *Int J Comput Assist Radiol Surg* 2015.

2. Schreiber G, McCrory DC: Performance characteristics of different modalities for diagnosis of suspected lung cancer: summary of published evidence. *Chest* 2003, 123(1 Suppl):115S-128S.

3. Yung RC: Tissue diagnosis of suspected lung cancer: selecting between bronchoscopy, transthoracic needle aspiration, and resectional biopsy. *Respir Care Clin N Am* 2003, 9(1):51-76.

4. Asano F: Application and Limitations of Virtual Bronchoscopic Navigation. In: Wang K-P, Mehta A, Turner J, eds. Flexible Bronchoscopy. In.: Chichester: John Wiley & Sons; 2012: 191-197.

5. Luo X, Kitasaka T, Mori K: Externally navigated bronchoscopy using 2-D motion sensors: dynamic phantom validation. *IEEE Trans Med Imaging* 2013, 32(10):1745-1764.

6. Reynisson PJ, Leira HO, Hernes TN, Hofstad EF, Scali M, Sorger H, Amundsen T, Lindseth F, Lango T: Navigated bronchoscopy: a technical review. *J Bronchology Interv Pulmonol* 2014, 21(3):242-264.

7. Merritt SA, Khare R, Bascom R, Higgins WE: Interactive CT-video registration for the continuous guidance of bronchoscopy. *IEEE Trans Med Imaging* 2013, 32(8):1376-1396.

8. Soper TD, Haynor DR, Glenny RW, Seibel EJ: In vivo validation of a hybrid tracking system for navigation of an ultrathin bronchoscope within peripheral airways. *IEEE Trans Biomed Eng* 2010, 57(3):736-745.

9. Luo X, Mori K: Robust Endoscope Motion Estimation Via an Animated Particle Filter for Electromagnetically Navigated Endoscopy. *Biomedical Engineering, IEEE Transactions on* 2014, 61(1):85-95.

10. Wegner I, Biederer J, Tetzlaff R, Wolf I, Meinzer H-P: Evaluation and extension of a navigation system for bronchoscopy inside human lungs. *Medical Imaging* 2007:65091H-65091H-65012.

11. Deguchi D, Ishitani K, Kitasaka T, Mori K, Suenaga Y, Takabatake H, Mori M, Natori H: A method for bronchoscope tracking using position sensor without fiducial markers. *Medical Imaging* 2007:65110N-65110N-65112.

12. Deguchi D, Feuerstein M, Kitasaka T, Suenaga Y, Ide I, Murase H, Imaizumi K, Hasegawa Y, Mori K: Real-time marker-free patient registration for electromagnetic navigated bronchoscopy: a phantom study. *International journal of computer assisted radiology and surgery* 2012, 7(3):359-369.

13. Mori K, Deguchi D, Kitasaka T, Suenaga Y, Hasegawa Y, Imaizumi K, Takabatake H: Improvement of Accuracy of Marker-Free Bronchoscope Tracking Using Electromagnetic Tracker Based on Bronchial Branch Information. In: *Medical Image Computing and Computer-Assisted Intervention, MICCAI 2008. Volume 5242*, edn. Edited by Metaxas D, Axel L, Fichtinger G: Springer Berlin Heidelberg; 2008: 535-542.

14. Feuerstein M, Sugiura T, Deguchi D, Reichl T, Kitasaka T, Mori K: Marker-free registration for electromagnetic navigation bronchoscopy under

625 respiratory motion. In: *Medical Imaging and Augmented Reality.* edn.: Springer; 2010: 237-246.

15. Hofstad EF, Sorger H, Leira HO, Amundsen T, Langø T: Automatic registration of CT images to patient during the initial phase of bronchoscopy: A clinical pilot study. *Medical physics (Lancaster)* 2014, 41(4).

630 16. Sorger H, Amundsen T, Hofstad EF, Langø T, Leira HO: A novel multimodal image guiding system for navigated endobronchial ultrasound (EBUS): human pilot study. . *Paper presented at the 3rd European Congress for Bronchology and Interventional Pulmonology (ECBIP), Barcelona, Spain,* 2015, 2015-04-23 - 2015-04-25.

635 17. Leira HO, Langø T, Hofstad EF, Sorger H, Amundsen T: Bronchoscope-induced Displacement of Lung Targets: First In Vivo Demonstration of Effect From Wedging Maneuver in Navigated Bronchoscopy. *Journal of Bronchology & Interventional Pulmonology* 2013, 20(3):206-212.

18. Horn BK: Closed-form solution of absolute orientation using unit
640 quaternions. *JOSA A* 1987, 4(4):629-642.

19. Smistad E, Elster AC, Lindseth F: GPU-Based Airway Segmentation and Centerline Extraction for Image Guided Bronchoscopy. *Norsk informatikkonferanse* 2012, 2012.

20. Zhang Y, Jing Y, Liang X, Xu G, Dong L: Dynamic lung modeling and tumor
645 tracking using deformable image registration and geometric smoothing. In: *CompIMAGE: 2012*; 2012: 215-220.

21. Luo X, Wan Y, He X, Mori K: Adaptive marker-free registration using a multiple point strategy for real-time and robust endoscope electromagnetic navigation. *Comput Methods Programs Biomed* 2015,
650 118(2):147-157.

22. Vijayan S, Reinertsen I, Hofstad EF, Rethy A, Hernes TA, Lango T: Liver deformation in an animal model due to pneumoperitoneum assessed by a vessel-based deformable registration. *Minim Invasive Ther Allied Technol* 2014, 23(5):279-286.

655